

Application Report

TMEM16A on Qube 384

A robust assay with precisely clamped internal Ca^{2+} and high seal resistances throughout the entire experiment

Summary

TMEM16A (ANO1) is a Ca^{2+} -activated Cl^- channel (CaCC) that is involved in a plethora of physiological and pathophysiological conditions. The channel was suggested as target for treatment of asthma, secretory diarrheas, and hypertension. TMEM16A is unique as its gating synergistically depends on voltage and cytosolic Ca^{2+} (Scudieri et al. 2012).

A robust TMEM16A assay was long awaited but progress was hampered as many automated patch clamp devices rely on the use of fluoride in the internal solution. Fluoride exhibits a very low solubility with calcium which means that calcium that is added to the internal solution to activate the channel has a strong tendency to precipitate, making it impossible to correctly adjust the calcium concentration.

We recently developed a novel approach to assay pharmacological inhibition of TMEM16A on Qube with following characteristics.

- Consistently high success rates (>80%)
- High degree of pharmacological reproducibility
- Very low run down and data spread

Introduction

Ca^{2+} -activated Cl^- channels were already described in the late 1980's but almost 30 years had to pass before its molecular identity was uncovered. In 2008, three groups independently identified TMEM16A that is also known as Anoctamin1, ANO1, DOG1, TAOS2 or ORAOV2 as CaCC (Caputo et al., 2008; Schroeder, Cheng, Jan, & Jan, 2008; Yang et al., 2008).

TMEM16A is involved in a wide area of physiological functions including neuronal excitability, smooth muscle cell contraction, epithelial fluid secretion and gastrointestinal motility. Moreover, TMEM16A was suggested as target for treatment of asthma,

secretory diarrheas, and hypertension (Pedemonte & Galletta, 2014). It was furthermore shown that TMEM16A plays a pivotal role in tumorigenesis in some tissues and may therefore prove itself as an interesting target in the treatment of cancer (Sauter et al., 2015) Interestingly, knock-out of TMEM16A caused severe tracheomalacia in mice followed by an early death (Rock et al., 2008).

TMEM16A gating critically depends on voltage and internal Ca^{2+} in a synergistic fashion, i.e. the half activation potential ($V_{1/2}$) shifts from +64 mV to -81 mV when intracellular Ca^{2+} is increased from 1 to 2 μM . The channel exhibits outward rectification of the steady state IV relationship that is due to activation at positive and deactivation at negative potentials. Interestingly, this rectification fades gradually when internal Ca^{2+} levels rise above 1 μM . TMEM16A gating was further reported to depend on the permeating ion with higher permeable anions, such as SCN^- , showing activation at more negative potentials compared to anions of lower permeability (Xiao et al., 2011). Sequence analysis of TMEM16A identified two calmodulin binding domains, suggesting a possible role of the accessory protein in TMEM16A gating. Although the exact relation is still subject to controversial discussion, it can be concluded that TMEM16A can be activated independently of calmodulin but the protein has likely a modulatory effect on the channel (Pang et al., 2014; Terashima et al., 2013).

Results and discussion

Figure 1 shows the success rates of 6 individual experiments (multi-hole QChips) and respective seal resistances. Filter criteria for success were defined as $C_{slow} \geq 5$ pF/cell; $I_{baseline} \geq 0.5$ nA/cell and $R_{membrane} \geq 0.1$ G Ω /cell. As described above, TMEM16A's IV relationship gradually linearizes when moving to higher intracellular Ca^{2+} values, i.e. a portion of channels is already activated at very negative potentials at ~ 1 μM free Ca^{2+} . This fact makes a correct determination of $R_{membrane}$ impossible. Therefore, $R_{membrane}$ was determined at the end of the experiment where cells were exposed to a high concentration (100 μM) of the TMEM16A inhibitor $CaCC_{inh}$ -A01 and almost all channels were inhibited. Our newly developed assay showed consistently high values for success rate (>80%) and $R_{membrane}$ (>0.4 G Ω /cell) between different runs and days.

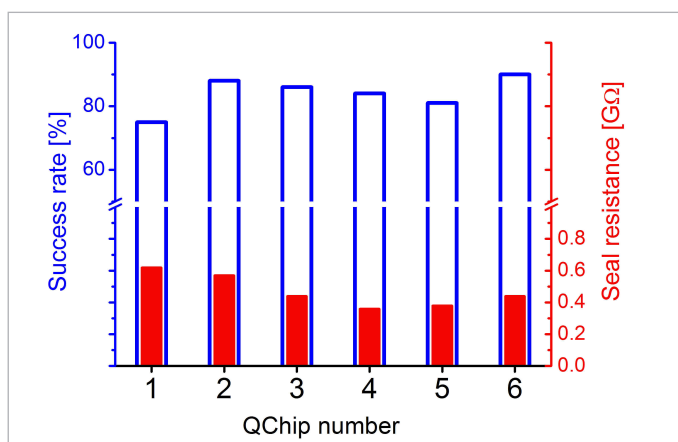


Fig. 1: Success rates (blue) and whole cell seal resistances (red) of 6 individual experiments (multi-hole QChips) performed on three different days. The filter criteria were defined as $C_{slow} \geq 5$ pF/cell; $I_{baseline} \geq 0.5$ nA/cell and $R_{membrane} \geq 0.1$ G Ω /cell.

Whole cell current traces in the presence and absence of ~ 1 μM free Ca^{2+} are shown in Figure 2. Currents were elicited using a 1 s long voltage step to +70 mV from a holding potential (V_{hold}) of -70 mV. After stepping back to V_{hold} , a voltage ramp from -90 mV to +90 mV was applied to the cells allowing direct assessment of current rectification. In line with TMEM16A characteristics reported in the literature, a step to +70 mV produced a time and voltage dependent current that reached a steady state plateau after a few 100 ms. IV relationships recorded using the ramp protocol exhibited a characteristic outward rectification that can be attributed to both the asymmetrical Cl^- gradient and the intrinsic voltage dependent gating at ~ 1 μM free internal Ca^{2+} . Application of the commonly used TMEM16A inhibitor $CaCC_{inh}$ -A01 at 100 μM almost completely inhibited this current. To show that the observed current is in fact Ca^{2+} -dependent, we omitted Ca^{2+} from the internal solution and a representative current trace is shown in Figure 2B. As expected, almost no currents were detected in this condition.

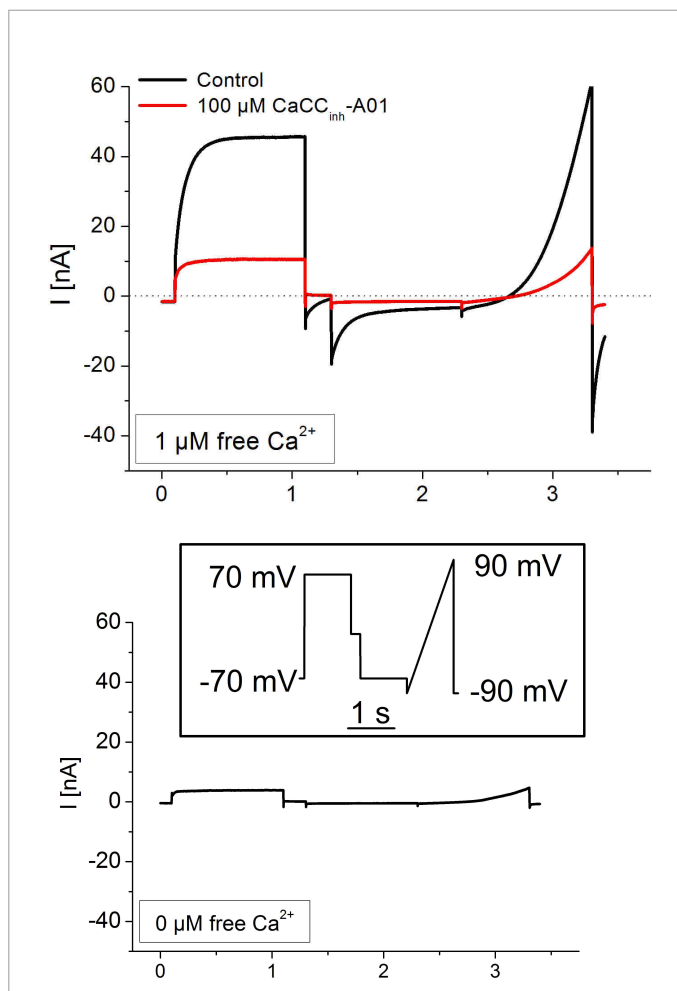


Fig. 2: Typical whole cell TMEM16A current traces. Currents were elicited using the voltage protocol shown in the insert. A: Current traces activated with approx. 1 μM free Ca^{2+} in the internal solution. Cells were subsequently exposed to the reference compound $CaCC_{inh}$ -A01 at 100 μM (red trace). B: Current traces recorded in a Ca^{2+} free solution.

To evaluate assay stability, we exposed cells to 0.1% DMSO and calculated run down (-up) at the end of a ~3 min liquid period (Figure 3 and Table 1). IT-plots measured at the steady state phase of the +70 mV step from individual measurement sites (multi-hole plate) are shown in Figure 3. Currents were stable during the entire course of the experiment. Application of 100 μM CaCC_{inh}-A01 almost completely inhibited TMEM16A current.

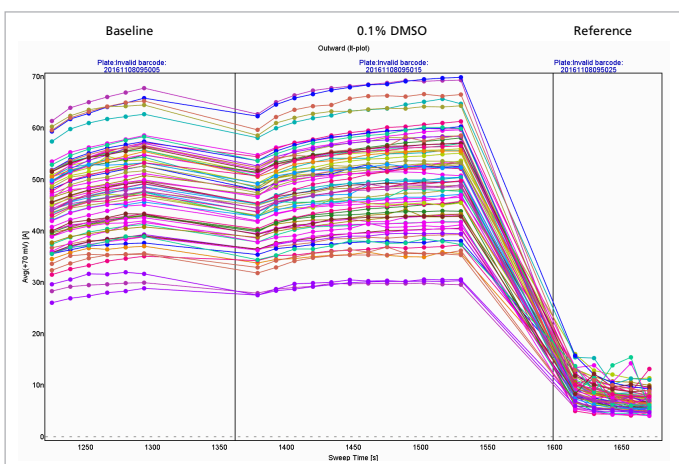


Fig. 3: IT - plot of the steady state TMEM16A current measured at $V=+70$ mV. Each trace represents a single measurement site. Following a saline period, cells were subjected to 0.1% DMSO. 100 μM CaCC_{inh}-A01 (last period) was used as a reference compound.

Table 2 summarizes IC₅₀ values from 4 independent runs. The obtained IC₅₀ values align well with values reported in the literature (Liu et al., 2014; Sung et al., 2016). Moreover, data showed low run-to-run variability.

Table 1: Summary current stability over time of four individual experiments (Run1-4). Run 1-2 were obtained using single-hole plates and Run 3-4 using multi-hole plates. Shown are mean +/- SD of n=79-90 cells.

	Run 1	Run 2	Run 3	Run 4
	Run down [%/min]	Run down [%/min]	Run down [%/min]	Run down [%/min]
0.1% DMSO	1 +/-2	-1 +/-1	1 +/-3	0+/-2

We used a set of 3 reference compounds, CaCC_{inh}-A01, benz-bromarone and niflumic acid to characterize the assay pharmacologically. Cells were exposed to 6 different concentration in a non-accumulated manner and dose response (DR) curves were determined using just n=1 per concentration. Such a set of DR curves is shown in Figure 4. Shown data was recorded using ~1 μM free Ca²⁺ in the pipette solution and drug effects were evaluated at the steady state phase of the +70 mV voltage step.

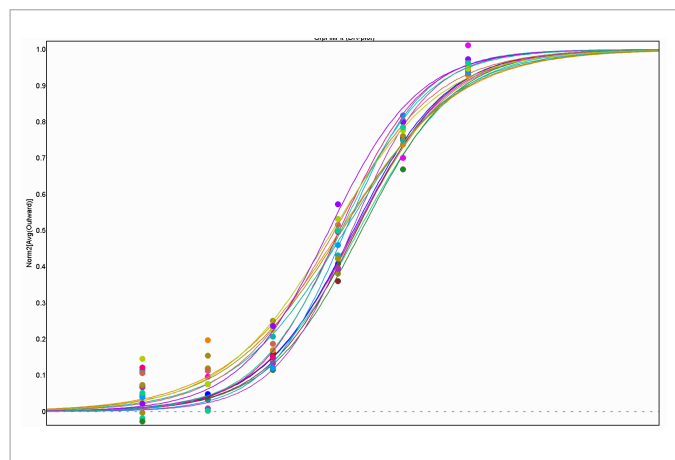


Fig. 4: Dose response curve of CaCC_{inh}-A01 with just n=1 per concentration. Data was normalized to the first saline period as baseline and reference compound as full response. Data was fitted using a Hill function.

Table 2: Summary of IC₅₀ values from 4 independent experiments (Run 1-4). Run 1-2 were obtained using single-hole plates and Run 3-4 using multi-hole plates. Values are mean values ± S.D. of individual DR curves with n=1 per concentration. N was between 6 and 16 for single-hole experiments and between 9 and 16 for multi-hole experiments.

	Single-hole		Multi-hole	
	Run 1	Run 2	Run 3	Run 4
	IC ₅₀ [μM]			
Benzbromaron	4±2	8±3	12±2	12±3
CaCC _{inh} -A01	7±3	7±4	13±2	11±3
Niflumic acid	16±7	21±6	19±5	25±7

Materials and Methods

Cells HEK293 cells stably expressing hTMEM16A kindly provided by SB Drug Discovery



Acknowledgement

HEK293 cells stably expressing hKCa3.1 kindly provided by Saniona A/S.

Author:

Daniel Sauter, Application scientist

In conclusion, we developed a robust TMEM16A assay on Qube that satisfies the requirements of a large compound screen or an extended medicinal chemistry program. Success rates were reasonably high consistently above 80%, but we expect that success rates can be even further optimized.

The assay showed high reproducibility and both biophysical as well as pharmacological characteristics are in line with literature values. A robust TMEM16A assay is also available for the QPatch.

References:

- Caputo, A., Caci, E., Ferrera, L., Pedemonte, N., Barsanti, C., Sondo, E., ... Galiotta, L. J. V. (2008). TMEM16A, a membrane protein associated with calcium-dependent chloride channel activity. *Science (New York, N.Y.)*, 322(5901), 590–4. <http://doi.org/10.1126/science.1163518>
- Liu, Y., Zhang, H., Huang, D., Qi, J., Xu, J., Gao, H., ... Zhang, H. (2014). Characterization of the effects of Cl⁻ channel modulators on TMEM16A and bestrophin-1 Ca²⁺ activated Cl⁻ channels. *Pflugers Archiv : European Journal of Physiology*, 1. <http://doi.org/10.1007/s00424-014-1572-5>
- Pang, C., Yuan, H., Ren, S., Chen, Y., An, H., & Zhan, Y. (2014). TMEM16A / B Associated CaCC : Structural and Functional Insights. *Protein & Peptide Letters*, 21(1), 94–99.
- Pedemonte, N., & Galiotta, L. J. V. (2014). Structure and function of TMEM16 proteins (anoctamins). *Physiological Reviews*, 94(2), 419–59. <http://doi.org/10.1152/physrev.00039.2011>
- Rock, J. R., Futtner, C. R., & Harfe, B. D. (2008). The transmembrane protein TMEM16A is required for normal development of the murine trachea. *Developmental Biology*, 321, 141–149. <http://doi.org/10.1016/j.ydbio.2008.06.009>
- Sauter, D. R. P., Novak, I., Pedersen, S. F., Larsen, E. H., & Hoffmann, E. K. (2015). ANO1 (TMEM16A) in pancreatic ductal adenocarcinoma (PDAC). *Pflugers Archiv : European Journal of Physiology*, 467, 1495–1508. <http://doi.org/10.1007/s00424-014-1598-8>
- Schroeder, B. C., Cheng, T., Jan, Y. N., & Jan, L. Y. (2008). Expression cloning of TMEM16A as a calcium-activated chloride channel subunit. *Cell*, 134(6), 1019–29. <http://doi.org/10.1016/j.cell.2008.09.003>
- Scudieri, P., Sondo, E., Ferrera, L., & Galiotta, L. J. V. (2012). The anoctamin family : TMEM16A and TMEM16B as calcium-activated chloride channels, 177–183. <http://doi.org/10.1113/expphysiol.2011.058198>
- Sung, T. S., O'Driscoll, K., Zheng, H., Yapp, N. J., Leblanc, N., Koh, S. D., & Sanders, K. M. (2016). Influence of intracellular Ca²⁺ and alternative splicing on the pharmacological profile of ANO1 channels. *American Journal of Physiology. Cell Physiology*, 1, ajpcell.00070.2016. <http://doi.org/10.1152/ajpcell.00070.2016>
- Terashima, H., Picollo, A., & Accardi, A. (2013). Purified TMEM16A is sufficient to form Ca²⁺-activated Cl⁻ channels. *Proceedings of the National Academy of Sciences of the United States of America*, 2013, 2–7. <http://doi.org/10.1073/pnas.1312014110>
- Xiao, Q., Yu, K., Perez-Cornejo, P., Cui, Y., Arreola, J., & Hartzell, H. C. (2011). Voltage- and calcium-dependent gating of TMEM16A/Ano1 chloride channels are physically coupled by the first intracellular loop. *Proceedings of the National Academy of Sciences of the United States of America*, 108(21), 8891–6. <http://doi.org/10.1073/pnas.1102147108>
- Yang, Y. D., Cho, H., Koo, J. Y., Tak, M. H., Cho, Y., Shim, W.-S., ... Oh, U. (2008). TMEM16A confers receptor-activated calcium-dependent chloride conductance. *Nature*, 455(7217), 1210–5. <http://doi.org/10.1038/nature07313>